

Electrochemical Characteristics, Thermal and Chemical Compatibility in the $\text{La}_{0.7}\text{Sr}_{0.3}\text{CoO}_3$ Electrode– γ -BIFEVOX Electrolyte System

E. S. Buyanova^a, R. R. Shafiqina^a, M. V. Morozova^a, Yu. V. Emel'yanova^a, V. V. Khisametdinova^a,
V. M. Zhukovskii^a, S. A. Petrova^b, and N. V. Tarakina^{c,d}

^a Ural Federal University, Yekaterinburg, Russia

^b Institute of Metallurgy, Ural Branch, Russian Academy of Sciences, Yekaterinburg, Russia

^c Institute of Solid-State Chemistry, Ural Branch, Russian Academy of Sciences, Yekaterinburg, Russia

^d Experimentelle Physik III, Physikalisches Institut und Wilhelm Conrad Röntgen-Research Center for Complex Material Systems, Universität Würzburg, Germany

Received April 10, 2012

Abstract—The electrochemical characteristics and compatibility of components of the electrode–electrolyte system, where the electrolyte is chosen to be γ -BIFEVOX compositions crystallizing in a stable tetragonal phase and the cathode material is chosen to be composite electrodes of composition $\text{La}_{0.7}\text{Sr}_{0.3}\text{CoO}_3 + \text{Bi}_4\text{V}_{1.7}\text{Fe}_{0.3}\text{O}_{11-\delta}$, were studied.

DOI: 10.1134/S0036023613050033

The family of solid electrolytes having the general formula $\text{Bi}_4\text{V}_{2-x}\text{M}_x\text{O}_{11-\delta}$, referred to as BIMEVOX in scientific literature, features rather high values of oxygen ion conductivity within a moderate-temperature range of 550–950 K. Studies of $\text{Bi}_4\text{V}_{2-x}\text{Fe}_x\text{O}_{11-\delta}$ (BIFEVOX) solid solutions established the concentration bounds and structural features of BIFEVOX polymorphs and ion transport characteristics depending on composition and temperature, and provided optimal conditions and methods for manufacturing ultrafine BIFEVOX powders [1–5].

Regardless of the preparation method, various researchers reported that solid solutions in the concentration range of $0.3 \leq x \leq 0.5$ have a tetragonal structure (space group $I4/mmm$). For low dopant concentrations ($x \leq 0.2$) [2], conductivity versus temperature curves feature typical consecutive phase transitions [$\gamma \rightarrow \beta$ (850 K) and $\beta \rightarrow \alpha$ (725 K)]; these transitions correspond to a change in structure ($I4/mmm \rightarrow Amam \rightarrow P-1$) and are accompanied with a change in activation energy of conduction in the solid solutions. For γ phases of the solid solutions (space group $I4/mmm$), the curves are linear plots, and the activation energies at high temperatures have values typical of BIMEVOX, namely, 0.2–0.4 eV. Transition to the ordered γ' phase upon lowering temperature is accompanied by an insignificant change in the slope of the $\log \sigma - 10^3/T$ curve and an increase in activation energy to 0.5–0.7 eV. All transitions observed in the conductivity curves correlate with changes in linear thermal expansion curves. In samples prepared by solution technologies for BIFEVOX, conductivity is always higher than in samples prepared by a solid-phase process.

Pena et al. [3] discovered that constant current conductivity decreases at relatively low temperatures (356–433 K) where the iron content increases, whereas the activation energy increases from 0.2 to 0.97 eV; these trends can serve as evidence for a significant contribution of oxygen ion conductivity to the overall conductivity of $\text{Bi}_4\text{V}_{2-x}\text{Fe}_x\text{O}_{11-y}$ ($0 \leq x \leq 0.9$, $0 \leq y \leq 1$).

A structural study of tetragonal $\text{Bi}_4\text{V}_{2-x}\text{Fe}_x\text{O}_{11-\delta}$ as a function of temperature and partial oxygen pressure discovered that this polymorph is stable over a wide range of thermodynamic parameters ($T = 298$ – 1073 K, $\log P_{\text{O}_2}$ [atm] = -0.68 to -18.0) [4, 5]. Under heating, a sample experiences only thermal expansion. As the oxygen partial pressure changes from 0.21 to 10^{-18} atm, the tetragonal BIFEVOX structure transforms to orthorhombic in a low-oxygen medium ($\log p_{\text{O}_2}$ [atm] < -14.0) at temperatures above 773 K. However, a sample does not undergo decomposition. The structural and thermal stability of BIFEVOX in air during long exposures (of at least two weeks at one temperature) over a temperature range of 723–1083 K with 50-K steps was evaluated earlier [6]. Structural alterations or the appearance of additional phases have not been found for γ -BIFEVOX phases over the entire temperature range of thermocycling.

Complex oxides of the BIMEVOX family were shown to be prone to attack with electrode materials [7–10]. In particular, platinum electrodes are attacked during long-term operation; gold electrodes are attacked to a lesser extent; and silver electrodes are completely dissolved or absorbed by the electrolyte during several operation cycles, thereby causing the closure of the circuit. In addition, gold electrodes cannot with-

Table 1. Metal component ratio and unit cell parameters in BIFEVOX

Synthesis method	x	Metal component ratio Bi : V : Fe		$a, \pm 0.001 \text{ \AA}$	$c, \pm 0.005 \text{ \AA}$	$V, \pm 0.7 \text{ \AA}^3$
		as-batch	AES			
Solid-phase synthesis	0.25	4.00 : 1.75 : 0.25	4.00 : 1.75 : 0.25	3.924	15.456	238.1
	0.3	4.00 : 1.70 : 0.30	4.00 : 1.70 : 0.30	3.925	15.511	238.6
PSC synthesis	0.25	4.00 : 1.75 : 0.25	4.00 : 1.75 : 0.25	3.919	15.472	239.6
	0.3	4.00 : 1.70 : 0.30	4.00 : 1.70 : 0.30	3.917	15.486	237.7

stand operation at high temperatures [7]. Diverse complex oxide materials are offered as an alternative. In particular, materials based on bismuth ruthenates of composition $\text{Bi}_2\text{Ru}_2\text{O}_7$ (pyrochlore structure) have been proposed for use for this purpose [8], as well as perovskite-like oxides $\text{La}_{1-x}\text{Sr}_x\text{MnO}_3$ and $\text{La}_{1-x}\text{Co}_x\text{MnO}_3$ [9, 10].

This study concerns an electrode–electrolyte system where the electrode is chosen to be a composite electrode of composition $\text{La}_{0.7}\text{Sr}_{0.3}\text{CoO}_3 + \gamma\text{-BIFEVOX}$ and the electrolyte is chosen to be a $\gamma\text{-BIFEVOX}$ composition, which crystallizes in tetragonal structure.

EXPERIMENTAL

$\text{Bi}_4\text{V}_{2-x}\text{Fe}_x\text{O}_{11-\delta}$ ($x = 0.25, 0.3$) solid solution samples were prepared by standard ceramic technology, by pyrolysis of polymer–salt compositions (PSC), and by mechanochemical activation [2]. The initial reagents used were Bi_2O_3 (high purity grade 13-3) or $\text{Bi}(\text{NO}_3)_3 \cdot 5\text{H}_2\text{O}$ (high purity grade 13-3), V_2O_5 (high purity grade 8-2), Fe_2O_3 (high purity grade 2-4) or $\text{Fe}(\text{NO}_3)_3 \cdot 9\text{H}_2\text{O}$ (pure for analysis), ammoniac, concentrated nitric acid (high purity grade 18-4), citric acid (pure grade), and polyvinyl alcohol 11/2 ($M \approx 30000\text{--}35000$). Vanadium oxide was dissolved in citric acid under heating in the ratio 1 : 3, or in nitric acid with addition of hydrogen peroxide (“extra” type). For the chosen values of the dopant cation index (x), the metal component ratio in the reaction mixtures was held at $\text{Bi} : \text{V} : \text{M} = 4 : (2 - x) : x$.

The mechanical treatment of oxides was performed with an AGO-2 planetary mill in the mode with the centrifugal factor $g = 60$ and a maximal exposure time of 23 min. Lanthanum strontium cobaltite of composition $\text{La}_{0.7}\text{Sr}_{0.3}\text{CoO}_3$ was prepared by PSC pyrolysis. The phase composition of products was monitored by X-ray diffraction (DRON-3 diffractometer, $\text{CuK}\alpha$ radiation; pyrolytic graphite monochromator on the reflected beam). Powder particle sizes were determined on a SALD-7101 Shimadzu dispersion analyzer. For use in electrochemical and thermal measurements, powders were compacted under a hydraulic press into tablets of 25 mm in diameter and rectangular stabs 25 mm in height, and then annealed at 1073 K. The criterion used to ascertain the density of the resulting ceramics was the ratio of the bulk density obtained by hydrostatic weighing and the X-ray density of the sample. Microstructure

analysis was performed using a JEOL JSM 6390LA scanning electron microscope equipped with a JED 2300 energy-dispersive microanalyzer. Elemental composition was determined by inductively coupled plasma/atomic emission spectroscopy (AES) on an iCAP 6500 Thermo Scientific spectrometer. Dilatometric studies of sintered samples were carried out on a DIL 402C Netzsch dilatometer. Electrical conductivity was studied by impedance spectroscopy (Elins Z-2000, Elins Z-350M impedance meter) between 973 and 473 K.

RESULTS AND DISCUSSION

BIFEVOX samples prepared by standard ceramic technology or the PSC method crystallize in tetragonal system (space group $I4/mmm$); the elemental compositions of the solid solutions as analyzed by two methods agree with each other and coincide with the as-batch composition (Table 1). The same result was obtained when BIFEVOX was synthesized by means of mechanochemical activation. Average particle sizes of powders prepared by different methods as determined by laser diffraction fall within a range of 0.5–10 μm . The porosity of the ceramics averages 3–5%.

Dilatometric analysis was used to detect possible phase transitions and determine linear thermal expansion coefficients of the ceramics. Figure 1 shows a representative curve showing the linear size for a sample of composition $\text{Bi}_4\text{V}_{1.75}\text{Fe}_{0.25}\text{O}_{11-\delta}$. One can see that no phase transitions occur in response to changing temperature, in agreement with X-ray diffraction studies. The small change in the slope observed for samples attested to be the tetragonal γ phase at room temperature corresponds to the $\gamma \leftrightarrow \gamma'$ order–disorder phase transition. The linear thermal expansion coefficient values calculated for BIFEVOX are $(17\text{--}18) \times 10^{-6} \text{ K}^{-1}$, and these values are comparable with the value for lanthanum strontium cobaltite ($\sim 20 \times 10^{-6} \text{ K}^{-1}$). In addition, the thermal stability of the prepared BIFEVOX solid solutions was studied in long-term heating–cooling cycles. Samples were consecutively annealed at temperatures of 723, 823, 923, 973, 1023, and 1083 K for two weeks at each stage and then in the reverse mode, and the slowly cooled samples were analyzed by X-ray diffraction. For $\text{Bi}_4\text{V}_{2-x}\text{Fe}_x\text{O}_{11-\delta}$ ($x = 0.25$ or 0.3) samples, which were the γ phase, no phase transitions were

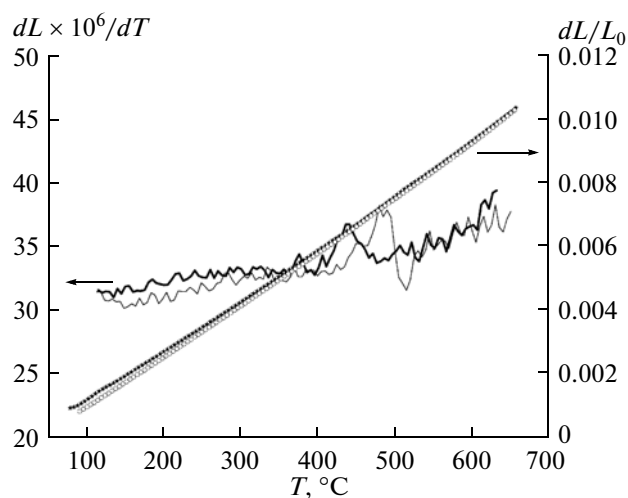


Fig. 1. Dilatometric curve for $\text{Bi}_4\text{V}_{1.75}\text{Fe}_{0.25}\text{O}_{11-\delta}$.

detected over the entire temperature range, and this implies the stability of this solid solution series.

Cho et al. [9] showed that, for oxygen concentration cells of BIMEVOX (where $M = \text{Cu}, \text{Ti}, \text{Zr}, \text{Nb}, \text{or Ta}$) solid electrolytes, the system with adjacent platinum electrodes operates worse than with $\text{La}_{0.6}\text{Sr}_{0.4}\text{Co}_{0.8}\text{Fe}_{0.2}\text{O}_3$ perovskite electrodes. Vincenzo et al. [8] studied the compatibility of $\text{Bi}_2\text{Ru}_2\text{O}_7$ electrodes with BICOVOX.10, BICUVOX.10, and BIZNVOX.10 electrolytes. Using X-ray powder diffraction, Vincenzo et al. showed that the electrode and electrolyte materials do not interact when annealed at 1073 K for 12 h. Furthermore, individual phases do not change their structures during this treatment.

In this study, composite electrodes of mixed compositions containing $\text{La}_{0.7}\text{Sr}_{0.3}\text{CoO}_3$ and $\text{Bi}_4\text{V}_{1.7}\text{Fe}_{0.3}\text{O}_{11-\delta}$ were used to reduce electrode overvoltage, because they have a greater interfacial surface area than for undoped lanthanum cobaltite alone. Similar systems have not been studied for the chemical and thermal compatibility of electrode–electrolyte.

In order to elucidate whether the electrolyte material (BIFEVOX) and the electrode material ($\text{La}_{0.7}\text{Sr}_{0.3}\text{CoO}_3$) interact with each other, we carried out an electron microscopic examination of compacted and annealed briquettes containing $\text{La}_{0.7}\text{Sr}_{0.3}\text{CoO}_3$ and $\text{Bi}_4\text{V}_{1.7}\text{Fe}_{0.3}\text{O}_{11-\delta}$ in various proportions, and carried out thermal anneals of powder mixtures of the same compositions with determination of the number of phases. The briquettes were manufactured by layer-by-layer compaction followed by annealing at 1073 K; the briquettes comprised the following layers: a $\text{La}_{0.7}\text{Sr}_{0.3}\text{CoO}_3 + \text{Bi}_4\text{V}_{1.7}\text{Fe}_{0.3}\text{O}_{11-\delta}$ composite layer with the ratio $\text{La}_{0.7}\text{Sr}_{0.3}\text{CoO}_3 : \text{Bi}_4\text{V}_{1.7}\text{Fe}_{0.3}\text{O}_{11-\delta} = 2 : 1$, which performed as the electrode; and a $\text{Bi}_4\text{V}_{1.7}\text{Fe}_{0.3}\text{O}_{11-\delta}$ electrolyte layer. The structure of a briquette is as follows: $\text{La}_{0.7}\text{Sr}_{0.3}\text{CoO}_3 + \text{Bi}_4\text{V}_{1.7}\text{Fe}_{0.3}\text{O}_{11-\delta} / \text{Bi}_4\text{V}_{1.7}\text{Fe}_{0.3}\text{O}_{11-\delta} / \text{La}_{0.7}\text{Sr}_{0.3}\text{CoO}_3 + \text{Bi}_4\text{V}_{1.7}\text{Fe}_{0.3}\text{O}_{11-\delta}$. Figures 2 and 3 show back-scattered

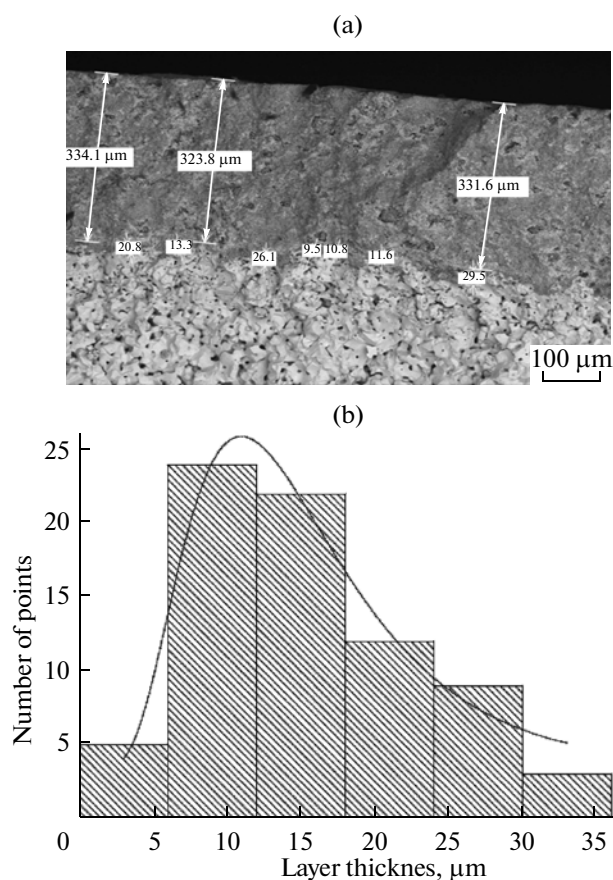


Fig. 2. Panel (a): a transverse cleave of a tablet (a general view). $\text{La}_{0.7}\text{Sr}_{0.3}\text{CoO}_3 + \text{Bi}_4\text{V}_{1.7}\text{Fe}_{0.3}\text{O}_{11-\delta} / \text{Bi}_4\text{V}_{1.7}\text{Fe}_{0.3}\text{O}_{11-\delta} / \text{La}_{0.7}\text{Sr}_{0.3}\text{CoO}_3 + \text{Bi}_4\text{V}_{1.7}\text{Fe}_{0.3}\text{O}_{11-\delta}$, $\text{La}_{0.7}\text{Sr}_{0.3}\text{CoO}_3 : \text{Bi}_4\text{V}_{1.7}\text{Fe}_{0.3}\text{O}_{11-\delta} = 2 : 1$. Panel (b): interlayer thickness.

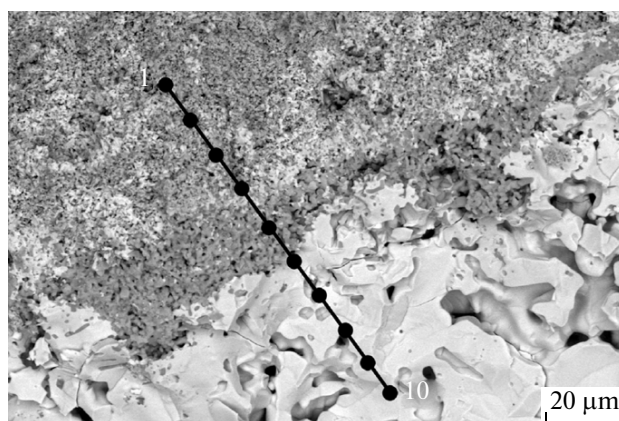


Fig. 3. Back-scattered electron image of a cleaved tablet. Dots along the line normal to the electrode/electrolyte interface indicate the sites where metal component concentrations were determined by energy-dispersive X-ray microanalysis.

electron microscopic images of a cleaved briquette where the composite component ratio is (2 : 1). Table 2 displays the metal component ratios derived from energy-dispersive X-ray microanalysis data where the spectra were measured consecutively at points along the line normal to the electrode/electrolyte interface (Fig. 3). Similar studies were carried out for a sample where the composite component ratio was 1 : 1.

From the data displayed, one can infer that an interlayer boundary is formed at the electrode/electrolyte interface, with a thickness ranging from 4 to 32 μm (average: 15 μm). This interlayer boundary comprises lanthanum, strontium, cobalt, vanadium, and (to a far smaller extent) bismuth. In order to determine the onset temperature of the reaction between $\text{La}_{0.7}\text{Sr}_{0.3}\text{CoO}_3$ and $\text{Bi}_4\text{V}_{1.7}\text{Fe}_{0.3}\text{O}_{11-\delta}$, mixtures of their powders taken in the same proportion were annealed. Each anneal stage was followed by X-ray diffraction attestation of the annealed samples. At temperatures starting with 973 K and higher, lanthanum strontium cobaltite and BIFEVOX react with each other to form such phases as lanthanum vanadate LaVO_4 and mixed bismuth strontium oxides (Fig. 4). At 873 K the reaction is yet not observed. It follows that lanthanum strontium cobaltites are undesirable for use as electrodes for BIFEVOX at temperatures above 973 K.

The temperature-dependent electrical conductivity of BIFEVOX with various electrodes in the range 973–473 K was studied by impedance spectroscopy. Figure 5 displays representative impedance spectra for $\text{Bi}_4\text{V}_{2-x}\text{Fe}_x\text{O}_{11-\delta}$ ($x = 0.3$) samples prepared by different methods, with different electrodes. The impedance spectra for cells with composite electrodes are identical in their shapes to the impedance spectra measured with platinum electrodes, and are described by the same equivalent circuits (Figs. 5a, 5b). The only what can be noticed is a decrease in semicircle radius and a shift of the impedance spectrum to higher frequencies for the systems with composite electrodes. However, the shape of the curve changes with temperature. At low temperatures, a semicircle is well seen and then disappears as temperature rises (Fig. 5c). An equivalent scheme of the cell that would correspond to the process occurring within a certain temperature range was chosen using Zview software (Version 2.6b, Scribner Associates).

For the low-temperature region, the scheme is a serial connection of resistors R_1 , R_2 , and R_3 with parallel-connected elements CPE1 and CPE2 (Fig. 5b). Resistor R_1 corresponds to the bulk conductivity of the sample; parallel connection of R_2 and CPE1 corresponds to grain-boundary transport; and parallel connection of R_3 and CPE2 corresponds to the occurrence of electrode processes. Thus, the sum $R = R_1 + R_2$ corresponds to the resistance of the sample with the proviso that the electrode processes are ignored.

The left-hand semicircles become degenerate as temperature rises; instead, a distorted semicircle appears likely due to electrode processes. This distorted

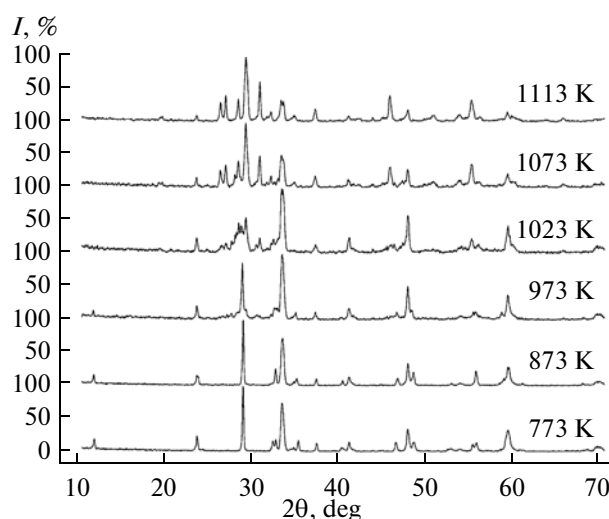


Fig. 4. X-ray diffraction patterns for mixtures of $\text{La}_{0.7}\text{Sr}_{0.3}\text{CoO}_3$ and $\text{Bi}_4\text{V}_{1.7}\text{Fe}_{0.3}\text{O}_{11-\delta}$ powder in the ratio 1 : 1, annealed at different temperatures.

semicircle is most likely a combination of at least two semicircles, which correspond, in the equivalent scheme, to a combination of resistors R_2 and R_3 with constant phase elements CPE2 and CPE1. In this case, resistor R_1 corresponds to the sum of the bulk resistance and intergrain resistance (Fig. 5c). The impedance measurements for $\text{Bi}_4\text{Fe}_x\text{V}_{2-x}\text{O}_{11-\delta}$ solid solutions were used to construct electrical conductivity versus temperature curves as displayed in Fig. 6 for samples of composition $\text{Bi}_4\text{Fe}_{0.3}\text{V}_{1.7}\text{O}_{11-\delta}$, which were prepared by different methods, using different electrodes. The general trend of polytherms for the test samples is typical of the BIMEVOX family [2]. A change in either electrode type or synthesis method does not change the slope of the conductivity versus temperature curve; the

Table 2. Metal component ratios (at %) derived from energy-dispersive X-ray microanalysis where spectra were recorded consecutively at points along the line normal to the electrode/electrolyte interface. The recording line is shown in Fig. 3. Datapoints corresponding to the interlayer boundary point are indicated in bold type

Da-ta-point	La	Sr	Co	V	Fe	Bi	Distance, μm
1	38.21	3.47	54.28			4.04	0.0
2	32.96	23.49	35.07			8.48	11.1
3	45.19	2.33	46.75			5.73	22.2
4	37.78	8.53	31.12		2.76	19.81	33.3
5	22.13	28.95	9.85	37.45		1.61	44.4
6	11.38	6.79		22.34		59.50	55.5
7			4.75	15.19	5.37	74.69	66.7
8			2.04	20.14	3.64	74.19	77.8
9				21.18	5.73	73.10	88.9
10				24.19	5.67	69.42	100.0

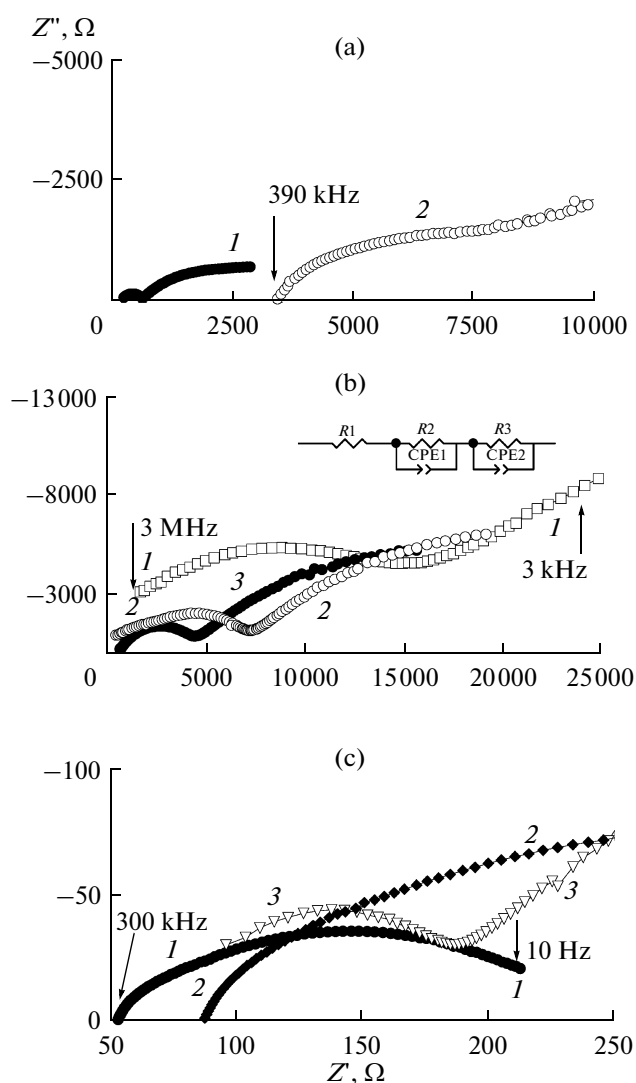


Fig. 5. Impedance spectra for cells containing $\text{Bi}_4\text{V}_{1.7}\text{Fe}_{0.3}\text{O}_{11-\delta}$ electrolyte prepared by different methods with two types of electrodes at different temperatures. Panel (a): 500°C: (1) mechanochemical synthesis, a cell with $\text{La}_{0.7}\text{Sr}_{0.3}\text{CoO}_3 + \text{Bi}_4\text{V}_{1.7}\text{Fe}_{0.3}\text{O}_{11-\delta}$ composite electrodes; (2) a cell with platinum electrodes. Panel (b): 400°C: (1) PSC pyrolysis, a cell with platinum electrodes; (2) PSC pyrolysis, a cell with $\text{La}_{0.7}\text{Sr}_{0.3}\text{CoO}_3 + \text{Bi}_4\text{V}_{1.7}\text{Fe}_{0.3}\text{O}_{11-\delta}$ composite electrodes; (3) solid-phase synthesis, a cell with $\text{La}_{0.7}\text{Sr}_{0.3}\text{CoO}_3 + \text{Bi}_4\text{V}_{1.7}\text{Fe}_{0.3}\text{O}_{11-\delta}$ composite electrodes). Panel (c): solid-phase synthesis, a cell with $\text{La}_{0.7}\text{Sr}_{0.3}\text{CoO}_3 + \text{Bi}_4\text{V}_{1.7}\text{Fe}_{0.3}\text{O}_{11-\delta}$ composite electrodes (1) 700, (2) 650, and (3) 600°C).

temperature coefficient is 0.7–0.8 eV for the range 950–750 K. The difference in absolute conductivity values arises from the variation in grain size depending on the synthesis method and the way in which the ceramics are formed, in correlation with the earlier studies [2, 4].

In summary, we have studied the compatibility of BIFVOX solid electrolytes with electrodes of composition $\text{La}_{0.7}\text{Sr}_{0.3}\text{CoO}_3$. We have proven that lanthanum strontium cobaltite reacts with BIFVOX at 973 K and

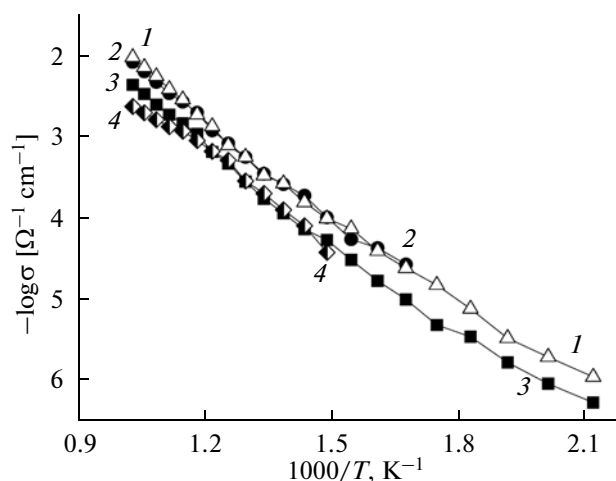


Fig. 6. Conductivity versus temperature for cells containing $\text{Bi}_4\text{V}_{1.7}\text{Fe}_{0.3}\text{O}_{11-\delta}$ electrolyte prepared by different methods, with two types of electrodes. For a cell with $\text{La}_{0.7}\text{Sr}_{0.3}\text{CoO}_3 + \text{Bi}_4\text{V}_{1.7}\text{Fe}_{0.3}\text{O}_{11-\delta}$ composite electrodes: (1) solid-phase synthesis, (2) PSC pyrolysis, and (3) mechanochemical synthesis. For a cell with platinum electrodes: (4) PSC pyrolysis.

higher temperatures. Below the onset temperature of the reaction, a change in electrode type (from platinum to a composite electrode of composition $\text{La}_{0.7}\text{Sr}_{0.3}\text{CoO}_3 : \text{Bi}_4\text{V}_{1.7}\text{Fe}_{0.3}\text{O}_{11-\delta} = 2 : 1$) does not give rise to a considerable change in electrochemical characteristics of the electrode–electrolyte system, and thereby it is advisable to study this system further.

ACKNOWLEDGMENTS

This work was supported by the Russian Fund for Basic Research (grant no. 12-03-00953).

REFERENCES

1. E. Garcia-Gonzalez, M. Arribas, and J. M. Gonzalez-Calbet, *Chem. Mater.* **13**, 96 (2001).
2. E. S. Buyanova, S. A. Petrova, Yu. V. Emel'yanova, et al., *Russ. J. Inorg. Chem.* **54**, 1193 (2009).
3. V. Pena, A. Rivera, and C. Leon, *Chem. Mater.* **14**, 1606 (2002).
4. V. M. Zhukovskii, E. S. Buyanova, Yu. V. Emel'yanova, et al., *Elektrokhimiya* **45**, 547 (2009).
5. M. V. Morozova, E. S. Buyanova, Ju. V. Emelyanova, et al., *Solid State Ionics* **192**, 153 (2011).
6. M. V. Morozova, E. S. Buyanova, S. A. Petrova, et al., *Elektrokhimiya* **47**, 475 (2011).
7. C. H. Hervoches, M. C. Steil, and R. Muccillo, *Solid State Sci.* **6**, 173 (2004).
8. E. Vincenzo, B. H. Luong, E. Di. Bartolomeo, et al., *J. Electrochem. Soc.* **153**, A2232 (2006).
9. H. S. Cho, G. Sakai, K. Shimano, and N. Yamazoe, *Sen. Act. B* **109**, 307 (2005).
10. E. S. Buyanova, Yu. V. Emel'yanova, M. V. Morozova, et al., *Elektrokhimiya* **46**, 810 (2010).

Translated by O. Fedorova